PNAS PLUS

α/β-Hydrolase domain-containing 6 (ABHD6) negatively regulates the surface delivery and synaptic function of AMPA receptors

Mengping Wei[a,1], Jian Zhang[a,1], Moye Jia[a,1], Chaojuan Yang[a,1], Yunlong Pan[a], Shuaiqi Li[a], Yiwen Luo[a], Junyuan Zheng[a], Jianguo Ji[a], Jianguo Chen[a], Xinli Hu[b], Jingwei Xiong[b], Yun Shi[c], and Chen Zhang[a,d,2]

[a]State Key Laboratory of Membrane Biology, School of Life Sciences, Peking University–IDG/McGovern Institute for Brain Research, Peking University, Beijing 100871, China; [b]Institute of Molecular Medicine, Peking University, Beijing 100871, China; [c]MOE Key Laboratory of Model Animal for Disease Study, Model Animal Research Center of Nanjing University, Nanjing, Jiangsu 210067, China; and [d]Beijing Institute of Collaborative Innovation, Beijing 100871, China

Edited by Thomas C. Südhof, Stanford University School of Medicine, Stanford, CA, and approved March 28, 2016 (received for review December 15, 2015)

In the brain, AMPA-type glutamate receptors are major postsynaptic receptors at excitatory synapses that mediate fast neurotransmission and synaptic plasticity. α/β-Hydrolase domain-containing 6 (ABHD6), a monoacylglycerol lipase, was previously found to be a component of AMPA receptor macromolecular complexes, but its physiological significance in the function of AMPA receptors (AMPARs) has remained unclear. The present study shows that overexpression of ABHD6 in neurons drastically reduced excitatory neurotransmission mediated by AMPA but not by NMDA receptors at excitatory synapses. Inactivation of ABHD6 expression in neurons by either CRISPR/Cas9 or shRNA knockdown methods significantly increased excitatory neurotransmission at excitatory synapses. Interestingly, overexpression of ABHD6 reduced glutamate-induced currents and the surface expression of GluA1 in HEK293T cells expressing GluA1 and stargazin, suggesting a direct functional interaction between these two proteins. The C-terminal tail of GluA1 was required for the binding between of ABHD6 and GluA1. Mutagenesis analysis revealed a GFCLIPQ sequence in the GluA1 C terminus that was essential for the inhibitory effect of ABHD6. The hydrolase activity of ABHD6 was not required for the effects of ABHD6 on AMPAR function in either neurons or transfected HEK293T cells. Thus, these findings reveal a novel and unexpected mechanism governing AMPAR trafficking at synapses through ABHD6.

ABHD6 | AMPA receptor | synapses | receptor trafficking

In the central nervous system, the amino acid glutamate is the major excitatory transmitter. The receptors for glutamate, which is critical for brain function, include ionotropic and metabotropic glutamate receptors. AMPA receptors (AMPARs) constitute one major class of ionotropic glutamate receptors that mediate fast excitatory synaptic transmission by binding glutamate released from presynaptic terminals. Mammals express four types of AMPAR subunits—GluA1, GluA2, GluA3, and GluA4—which are encoded by *Gria1*, *Gria2*, *Gria3*, and *Gria4*, respectively (1, 2). Mature AMPARs are tetramers composed of GluA1–4 (3). The subunit composition determines their kinetics and pharmacological properties (4–6). Except for these pore-forming subunits, native AMPARs are thought to be macromolecular complexes associated with a variety of auxiliary proteins, including transmembrane AMPA receptor regulatory proteins, cornichons, Gsg1l, syndig1, and CKAMP44 (7–20). Recently, a high-resolution proteomics analysis revealed 21 additional proteins associated with native AMPAR core subunits (21). The α/β-hydrolase domain-containing 6 (ABHD6) enzyme, which is implicated in the hydrolysis of 2-arachidonoylglycerol (2-AG), was found to be a component of native AMPA receptor complexes. Interestingly, ABHD12 was also found in these complexes. These observations led to a tempting hypothesis: 2-AG signaling might be directly involved in the function and trafficking of the AMPA receptor.

ABHD6 and ABHD12 belong to the α/β-hydrolase family, which comprises at least 15 genes (22, 23). ABHD6 has been detected in various tissues, including the brain, liver, kidney, and pancreatic islets (24, 25). In the brain, ABHD6 localizes predominantly to postsynaptic sides, whereas the other major 2-AG hydrolase, monoacylglycerol lipase (MAGL), is found mainly in axons and presynaptic terminals (26–29). In the human cortex, ABHD6 mRNA expression begins in the neonatal period and increases until adulthood (30). Previous studies have identified ABHD6 as a lipase (25, 31). ABHD6, MAGL, and ABHD12 were found to be major enzymes in the brain, hydrolyzing >99% of endocannabinoid 2-AG in a substrate- and isoform-specific manner (32, 33). Knockdown of ABHD6 with antisense oligonucleotides in the liver, white adipose tissue, and kidney tissue exerted a protective effect against high-fat diet-induced obesity in mice (34). Inhibition of the ABHD6 lipase with WWL70, a specific inhibitor of ABHD6 lipase activity, or by knockout of ABHD6 specifically in β-cells increased glucose-stimulated insulin secretion in pancreatic β-cells, implying a role for ABHD6 in regulating exocytosis (24). Many previous studies on the role of ABHD6 in brain functioning have focused on the contributions of 2-AG and endocannabinoid-related signaling. For example, depolarization-induced suppression of excitation (DSE) or inhibition (DSI) are two forms of synaptic modulation that

Significance

AMPA receptors (AMPARs) are major postsynaptic receptors that mediate fast excitatory neurotransmission and synaptic plasticity. The proper functioning of AMPARs is essential for brain function; AMPAR dysfunction can cause multiple neurologic disorders, including autism. Native AMPARs are macromolecular complexes associated with a variety of auxiliary proteins, including α/β-hydrolase domain-containing 6 (ABHD6), which was recently identified. However, the physiological significance of the ABHD6–AMPAR association has not been investigated. Here, using both loss-of-function and gain-of-function approaches, we show that ABHD6 negatively regulates the surface delivery and synaptic function of AMPARs in neurons. The cytoplasmic tail of GluA1, but not the hydrolase activity of ABHD6, is essential for this functional interaction. Thus, these new findings expand our understanding of the molecular mechanisms governing AMPAR trafficking in the brain.

Author contributions: M.W., J. Zhang, M.J., J.J., J.C., X.H., J.X., Y.S., and C.Z. designed research; M.W., J. Zhang, M.J., C.Y., Y.P., Y.L., and J. Zheng performed research; M.W., J. Zhang, M.J., C.Y., Y.P., S.L., and J. Zheng analyzed data; and C.Z. wrote the paper.

The authors declare no conflict of interest.

This article is a PNAS Direct Submission.

Freely available online through the PNAS open access option.

[1]M.W., J. Zhang, M.J., and C.Y. contributed equally to this work.

[2]To whom correspondence should be addressed. Email: ch.zhang@pku.edu.cn.

This article contains supporting information online at www.pnas.org/lookup/suppl/doi:10.1073/pnas.1524589113/-/DCSupplemental.

depend on 2-AG and endocannabinoid signaling (35–40). The brain-penetrant ABHD6 inhibitor, WWL123, did not affect DSE in cerebellar slices, whereas genetic inactivation of MAGL resulted in prolonged DSE at Purkinje cell synapses in granule cells or the inferior olivary nucleus (41). WWL123 had no effects on DSI or DSE in autapse preparations (28, 42), and overexpression of mouse ABHD6 or ABHD12 in hippocampal autapse preparations had no effects on the kinetics of DSE (43). In layer 5 of prefrontal cortical slices, blocking ABHD6 or MAGL activity with WWL70 or JZL184, respectively, induced endocannabinoid-dependent long-term depression via subthreshold stimulation of layer 2 neurons (29). Furthermore, these effects were blocked by AM251, a cannabinoid receptor type 1 blocker. In contrast, treatment with either WWL70 or JZL184 did not significantly alter the kinetics of DSE at the same synapse. Serine hydrolase inhibitors are used for the treatment of many diseases, including cognitive dementia, obesity, and diabetes. ABHD6 is considered an attractive therapeutic target for manipulating 2-AG signaling (44–46). Chronic WWL70 treatment after traumatic brain injury exerted a neuroprotective effect by increasing the levels of 2-AG in the brain (47). Pretreating mice with WWL123, another brain-penetrant ABHD6 inhibitor, alleviated epileptic symptoms during pentylenetetrazole-induced seizures, and this blockade was absent in the presence of γ-aminobutyric acid type A receptor antagonists (48).

Thus, multifarious effects and roles have been associated with ABHD6 in various systems. However, it is not clear whether the newly identified association between ABHD6 and AMPARs has physiological relevance. Similarly, whether ABHD6 affects the function of AMPARs via the 2-AG signaling pathway or by a more direct action has not yet been tested. The present study explored the role of ABHD6 in the function of AMPARs using electrophysiological recordings in primary hippocampal neurons, acute hippocampal slices, and transfected HEK293T cells using both gain-of-function and loss-of-function assays.

Results

Overexpression of ABHD6 Inhibited AMPAR-Mediated Synaptic Transmission and the Surface Expression of GluA1 in Hippocampal Neurons. AMPARs are major postsynaptic receptors at excitatory synapses in the brain. ABHD6 was highly expressed in cultured neurons and in the brain, and its expression levels increased during development and remained stable throughout adulthood (Fig. S1). To assess whether ABHD6 affected AMPAR-mediated synaptic transmission, neurons were transfected with GFP or ABHD6 fused to P2A-GFP, such that less than 1% of the neurons were transfected, and the synaptic responses of the transfected neurons identified via GFP fluorescence were recorded (49). To ensure that the neurons selected for recording indeed expressed all of the desired constructs, we transfected hippocampal neurons with three separate vectors encoding the fluorescent markers GFP (green fluorescent protein), BFP (blue fluorescent protein), and tdTomato (tdTomato fluorescent protein). Consistent with other studies using similar transfection strategies (49, 50), 94.44% (102 of 108 neurons from three independent transfections) of the transfected neurons expressed the three markers simultaneously (Fig. S2). Moreover, the coexpression percentages of pairs of fluorescent markers in the same experiments were 95.24% (BFP/GFP), 94.44% (BFP/tdTomato), and 99.21% (GFP/tdTomato), confirming the reliability of our cotransfection method.

Our results showed that the transfection of ABHD6 caused an ∼10-fold decrease in the frequency of miniature excitatory postsynaptic currents (mEPSCs) and an ∼1.5-fold decrease in the amplitudes of mEPSCs (Fig. 1*A*). The transfection of ABHD6 into neurons had no effects on membrane capacitance (control: 57.01 ± 2.457 pF; ABHD6: 57.71 ± 2.34 pF) or resistance (control: 379 ± 14 MΩ, n = 175 cells/23 cultures; ABHD6: 350 ± 11 MΩ, n = 178/23) compared with the GFP-transfected neurons. To ensure that the observed effects were specific to the transfected neurons, mEPSCs in transfected and nontransfected neighboring neurons were measured on the same coverslip. Only the transfected neurons expressing ABHD6 showed impaired mEPSCs (Fig. 1*B* and Fig. S3). An analysis of the rising slope and decay time course of the mEPSCs showed that overexpression of ABHD6 significantly decreased the rising slope of the mEPSCs and increased the decay τ (Fig. 1*C*), showing that ABHD6 affected the kinetics of these mEPSCs. Recordings of the evoked synaptic responses (EPSCs) revealed a similar decrease in the amplitudes of the EPSCs (Fig. 1*D*). Furthermore, ABHD6 overexpression significantly decreased the EPSCs induced by hypertonic sucrose, which induces the release of all readily releasable vesicles (Fig. 1*E*). Measurements of the somatic ligand-induced

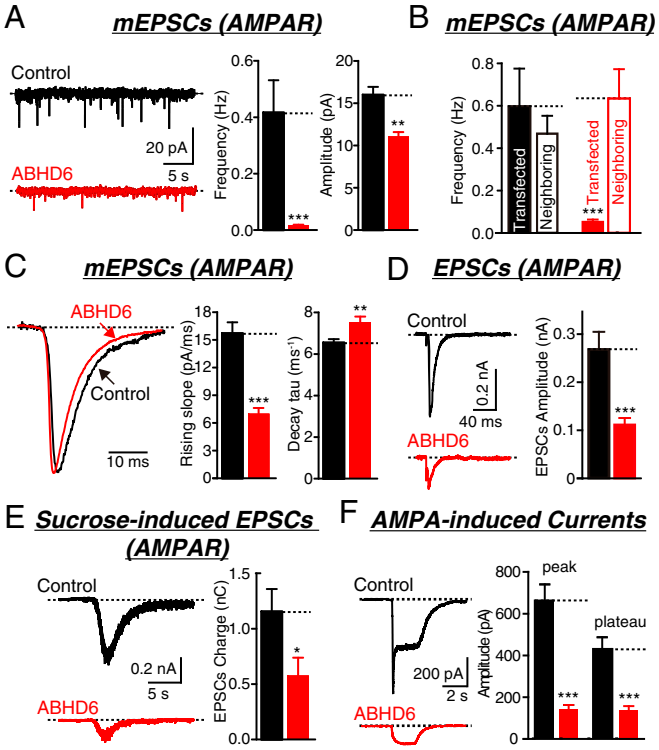

Fig. 1. Cell-autonomous inhibition of AMPAR-mediated postsynaptic currents by ABHD6 overexpression. All data are from cultured hippocampal neurons transfected with either an empty vector (control) or a vector encoding ABHD6-2A-GFP in electrophysiological experiments. (*A*) Representative traces (*Left*) and summary graphs of the frequencies (*Center*), and amplitudes (*Right*) of mEPSCs recorded in 1 μM tetrodotoxin (TTX) and 0.1 mM PTX (control: n = 30 cells/3 cultures; ABHD6: n = 35/3, frequency: ***P < 0.001, amplitude: **P < 0.01). (*B*) Summary graphs of the frequencies of mEPSCs recorded from transfected and neighboring (nontransfected) neurons (control: n = 32 pairs, frequency: P > 0.05; ABHD6: n = 29 pairs, frequency: ***P < 0.001). (*C*) Representative traces (*Left*) and summary graphs of the rising slope (*Center*) and decay τ (*Right*) of normalized traces of mEPSCs (rising slope: control: 57/6, ABHD6: 20/6, ***P < 0.001; decay τ: control: 57/6; ABHD6: 20/6, **P < 0.01). (*D*) Representative traces (*Left*) and summary graphs of the amplitudes (*Right*) of action potential-evoked EPSCs recorded in 0.1 mM PTX (control: n = 43/4; ABHD6: n = 43/4, ***P < 0.001). (*E*) Representative traces (*Left*) and mean charge transfer (*Right*; integrated over 60 s) of EPSCs elicited by hypertonic sucrose (0.5 M for 30 s; control: n = 13/4; ABHD6: n = 13/4, *P < 0.05). (*F*) Representative traces (*Left*) and peak amplitudes and plateaus (*Right*) of currents induced by the application of 200 μM AMPA to hippocampal neurons transfected with ABHD6 or a control vector recorded in 1 μM TTX, 0.1 mM PTX, and 50 μM AP5 (peak: control: n = 24/3, ABHD6: n = 27/3, ***P < 0.001; plateau: control: n = 22/3, ABHD6: n = 24/3, ***P < 0.001).

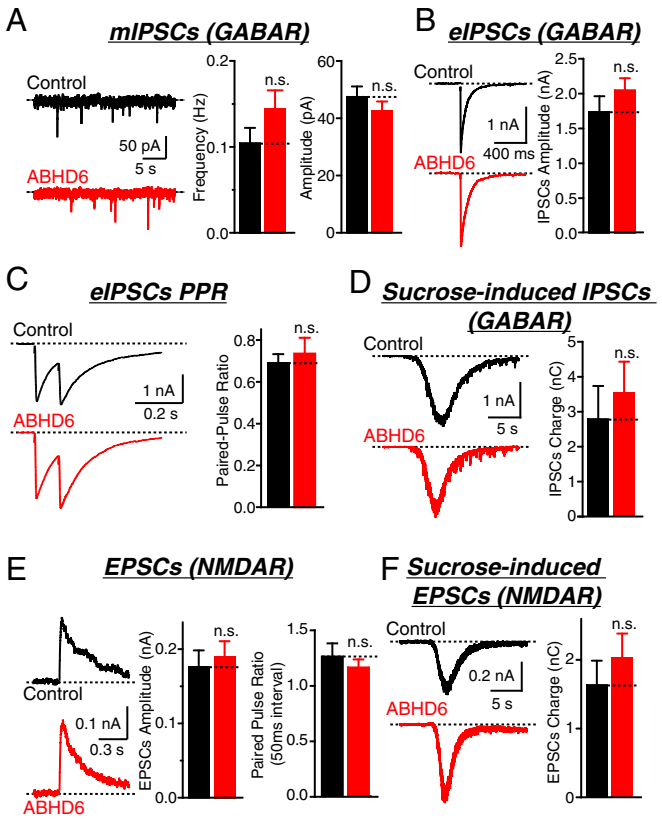

Fig. 2. ABHD6 has no effects on GABAergic or NMDAR-mediated postsynaptic currents. All data are from cultured hippocampal neurons transfected with either an empty vector (control) or a vector encoding ABHD6-2A-GFP in electrophysiological experiments. (*A*) Representative traces (*Left*) and summary graphs of the frequencies (*Center*) and amplitudes (*Right*) of mIPSCs recorded in 10 μM CNQX (control: $n = 31/3$; ABHD6: $n = 30/3$, frequency: $P > 0.05$, amplitude: $P > 0.05$; ns, not significant). (*B*) Representative traces (*Left*) and summary graphs of the amplitudes (*Right*) of action potential-eIPSCs recorded in 10 μM CNQX (IPSCs: control: $n = 23/3$; ABHD6: $n = 31/3$, $P > 0.05$). (*C*) Representative traces (*Left*) and paired-pulse ratio (*Right*) of IPSCs evoked by two closely spaced action potentials (100-ms interval, control: $n = 23/3$; ABHD6: $n = 32/3$, $P > 0.05$). (*D*) Representative traces (*Left*) and mean charge transfer (*Right*; integrated over 60 s) of IPSCs elicited by hypertonic sucrose (0.5 M for 30 s; IPSCs: control: $n = 9/3$; ABHD6: $n = 8/3$, $P > 0.05$). (*E*) Representative traces (*Left*) and summary graphs of the amplitudes (*Center*) of action potential-evoked EPSCs recorded in 100 μM PTX and 10 μM CNQX at +40 mV, paired-pulse ratio (*Right*) of EPSCs evoked by two closely spaced action potentials. (NMDAR: control: $n = 41/4$; ABHD6: $n = 42/4$, $P > 0.05$; paired pulse ration: 50-ms interval, control: control: $n = 26/3$; ABHD6: $n = 29/3$, $P > 0.05$).

currents elicited by puffing 200 μM of AMPA revealed a similar robust reduction in the amplitude (Fig. 1*F*). To examine whether ABHD6 specifically affected AMPAR-mediated synaptic transmission, synaptic responses mediated by NMDA receptors (NMDARs) or GABA A receptors (GABAARs) at the hippocampal synapses were monitored. ABHD6 caused no change in either the frequency or the amplitude of GABAAR-mediated miniature inhibitory postsynaptic currents (mIPSCs). No changes were observed in evoked IPSCs (eIPSCs) or the paired-pulse ratio (Fig. 2 *A*–*C*). IPSCs induced by hypertonic sucrose were also normal in ABHD6-transfected neurons (Fig. 2*D*), showing that GABAAR-mediated synaptic transmission was intact in the ABHD6-overexpressing neurons. NMDARs, another type of ionotropic glutamate receptor, colocalize with AMPARs at mature glutamatergic synapses (51, 52). The opening of NMDARs requires simultaneous glutamate binding and removal of magnesium blockade at rest (53). AMPARs and GABARs were pharmacologically blocked with 6-cyano-7-nitroquinoxaline-2,3-dione (CNQX) and picrotoxin (PTX), respectively, and the action potential (AP)-induced synaptic transmission mediated by NMDARs at excitatory synapses was recorded at a membrane potential of +40 mV in the absence of extracellular magnesium. The results showed that NMDAR-mediated AP-induced or hypertonic sucrose-induced EPSCs were not affected by the postsynaptic overexpression of ABHD6 (Fig. 2 *E* and *F*). These observations clearly demonstrated that ABHD6 overexpression specifically affected AMPAR-mediated synaptic transmission at the excitatory synapses.

To test whether ABHD6 overexpression alters the synaptic AMPAR levels, we measured the surface and total GluA1 levels in transfected neurons using quantitative immunocytochemistry. The results revealed that ABHD6 reduced the surface expression levels of GluA1, as reflected by a decreased number of $GluA1^{surface+}$ puncta in nonpermeabilized neurons (Fig. 3*A*). In contrast, ABHD6 had no effect on $GluA1^{total+}$ puncta at postsynaptic terminals in permeabilized neurons (Fig. 3*B*). The numbers of $vGlut1^{+}$ and $PSD\text{-}95^{+}$ puncta were also normal in ABHD6-transfected dendrites (Fig. 3 *C* and *D*). In addition, the numbers of $NMDAR^{+}$ and $GAD65^{+}$ puncta were both normal (Fig. S4), suggesting that ABHD6 specifically interacts with AMPARs at synapses and reduces the surface expression of postsynaptic AMPARs.

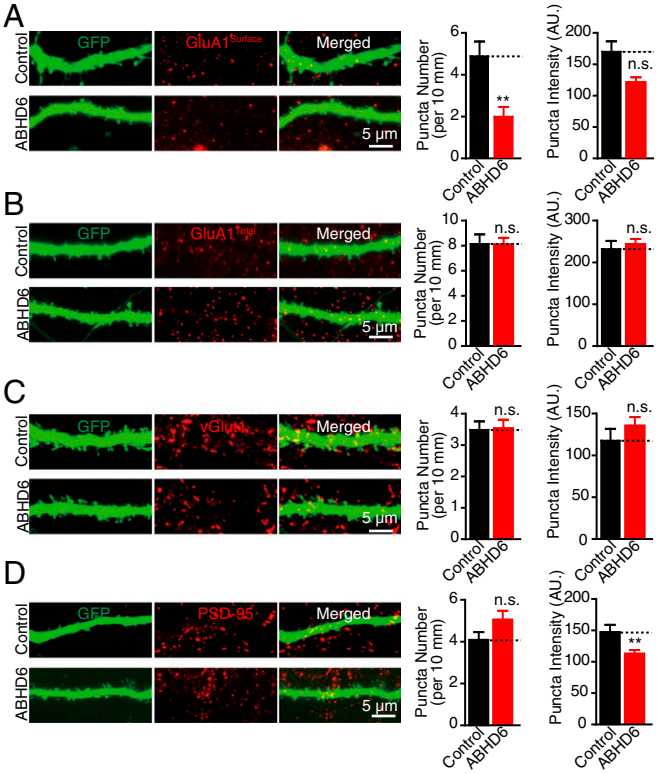

Fig. 3. Postsynaptic expression of ABHD6 reduced surface GluA1 levels. Measurements of the synaptic signals of surface GluA1 (*A*), total GluA1 (*B*), vGlut1 (*C*), and PSD-95 (*D*) in neurons expressing ABHD6 or the control. The transfected neurons were stained with antibodies against GluA1 (either permeabilized in *B* or nonpermeabilized in *A*), vGlut1, and PSD-95. The panels show representative images (*Left*) and quantification of the puncta (*Right*) (puncta number: *A*: control: $n = 37/3$, ABHD6: $n = 33/3$, $^{**}P < 0.01$; *B*: control: $n = 40/3$; ABHD6: $n = 42/3$, $P > 0.05$; *C*: control: $n = 30/3$; ABHD6: $n = 43/3$, $P > 0.05$; *D*: control: $n = 16/3$; ABHD6: $n = 22/3$, $P > 0.05$; puncta intensity: *A*: control: $n = 37/3$, ABHD6: $n = 26/3$, $P > 0.05$; *B*: control: $n = 41/3$; ABHD6: $n = 43/3$, $P > 0.05$; *C*: control: $n = 30/3$; ABHD6: $n = 42/3$, $P > 0.05$; *D*: control: $n = 16/3$; ABHD6: $n = 20/3$, $^{**}P < 0.01$).

To examine the physiological importance of the observed effects, we examined synaptic currents using whole-cell recordings in acute hippocampal brain slices injected with adeno-associated virus (AAV) expressing either ABHD6 or GFP as a control. By recording the synaptic currents from transfected and neighboring neurons, we found that AMPAR eEPSCs were not changed between control GFP and neighboring untransfected neurons (Fig. 4 *A*, *1*). We simultaneously recorded eEPSCs from ABHD6-transfected and neighboring untransfected neurons and found that the amplitude was significantly reduced by ~57 ± 14% (Fig. 4 *A*, *2*), suggesting that ABHD6 affects constitutive AMPAR trafficking. Next, to investigate whether ABHD6 affect activity-dependent receptor trafficking at synapses, we measured long-term potentiation (LTP) in the hippocampal Schaffer collateral pathway in acute brain slices injected with AAVs expressing ABHD6. After recording a 5-min baseline, a pairing protocol (2-Hz stimulus for 90 s while clamping the postsynaptic neuron at 0 mV) (54) was used to induce LTP. We found that overexpression of ABHD6 resulted in decreased LTP compared with uninfected neurons (Fig. 4*B*), showing that ABHD6 affects AMPA receptor levels during induction and maintenance of LTP. Taken together, our results demonstrate that ABHD6 affected AMPAR function in both cultured neurons and hippocampal slices.

Inactivation of ABHD6 by CRISPR/Cas9 or shRNAs Increased AMPAR-Mediated Synaptic Transmission in Hippocampal Neurons. Next, we examined the effects of ABHD6 on the AMPAR-mediated synaptic transmission using two different loss-of-function approaches. First, the CRISPR/Cas9 system was used to delete ABHD6 in cultured hippocampal neurons. The CRISPR/Cas9 method has proven to be a powerful method to knock out genes in both cells and animals (55–65). Recently, the complete functional deletion of synaptic proteins, including the GluN1 subunit of the NMDA receptor and the GluA2 subunit of the AMPA receptor, was reported in hippocampal neurons (50). Thus, a subgenomic RNA (sgRNA) targeting the second exon of mouse ABHD6 was constructed, and its efficiency in reducing the expression of ABHD6 in transfected HEK293T cells was examined (Fig. 5*A*). A Western blot of ABHD6 in the transfected HEK293T cells showed a significant and specific reduction in the expression of ABHD6 in the CRISPR^{ABHD6} group compared with a control group (Fig. 5*B* and Fig. S5). The transfection of CRISPR^{ABHD6} into hippocampal neurons at 10 d in vitro (DIV) increased both the frequency of mEPSCs and the amplitude of the evoked EPSCs, and this effect was abolished by coexpressing an ABHD6 rescue construct carrying a 2A-GFP fluorescent marker for visualization (Fig. 5 *C* and *D*). Second, two shRNAs (sh37 and sh49), which were previously shown to inactivate the expression of ABHD6 by 37% and 49%, respectively (29), were transfected, and their effects on excitatory synaptic transmission in cultured hippocampal neurons were examined. The results showed that the transfection of both shRNAs targeting ABHD6 increased the frequency of mEPSCs (Fig. 5*E*), similar to the synaptic effects observed in the CRISPR-mediated deletion experiments. Additionally, the overexpression of a full-length ABHD6 cDNA together with shRNAs reversed the knockdown effects on mEPSCs. Furthermore, knockdown of ABHD6 using an AAV expressing sh49 caused an almost twofold increase in the amplitude of evoked EPSCs in the CA3-CA1 synapses in the acute hippocampal slices (Fig. 5*F*). Thus, these results clearly indicate that inactivation of ABHD6 in neurons increases AMPAR-mediated synaptic transmission.

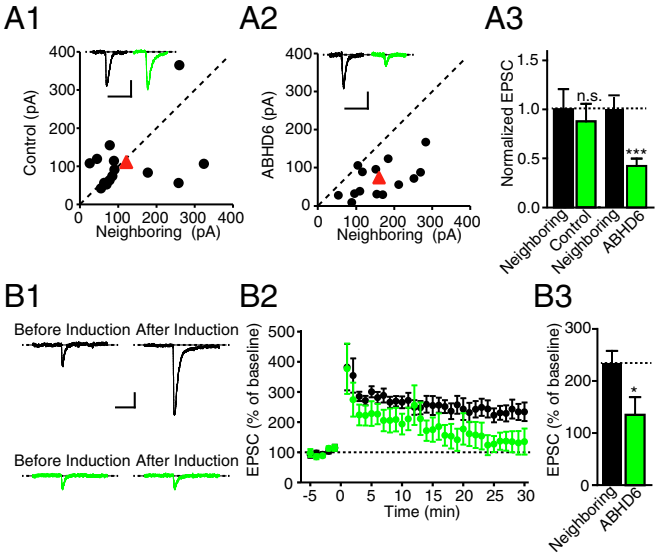

Fig. 4. Overexpression of ABHD6 in hippocampal slices impaired AMPAR-mediated EPSCs and pairing LTP. (*A*) The plot of the amplitude of AMPAR EPSCs of cells in acute hippocampal slices infected with AAVs expressing GFP (*A*, *1*) or ABHD6 (*A*, *2*) against the amplitudes of neighboring uninfected cells, and summary graphs of the normalized AMPAR EPSCs amplitude (*A*, *3*). (*Inset*) Representative traces of synaptic responses during single AP stimulus (Scale bars in *A*, *1* and *A*, *2*: 50 pA, 100 ms; control: $n = 14$, $P > 0.05$; ABHD6: $n = 14$; $^{***}P < 0.001$). (*B*) Representative traces before (*Left*) and after (*Right*) LTP induction (*B*, *1*), and LTP induced by a paring protocol in neurons infected with an AAV expressing ABHD6 compared with the uninfected cells (*B*, *2*), and summary graph of the average normalized amplitude (*B*, *3*) of EPSCs 25–30 min after the induction of LTP. (Scale bars in *B*, *1*: 50 pA, 100 ms; control: $n = 9$; ABHD6: $n = 9$; $^{*}P < 0.05$).

Overexpression of ABHD6 Decreased Glutamate-Induced Currents and the Surface Expression of GluA1 in HEK293T Cells Expressing GluA Subunits. To examine whether the observed neuronal phenotypes reflected a direct functional interaction between ABHD6 and AMPARs, we examined the effects of ABHD6 overexpression on glutamate-induced currents recorded from HEK293T cells transfected with various AMPAR subunits, either alone or together with stargazin (7, 8). Stargazin is a four-transmembrane protein associated with AMPARs in vivo, which plays a critical role in delivering AMPARs to the plasma membrane (10, 16, 66). The currents elicited under all conditions were AMPAR-specific; HEK293T cells without GluA transfection showed no detectable currents (Fig. S6). Compared with GFP-transfected cells, overexpression of human ABHD6 fused to P2A-GFP significantly reduced the amplitude of glutamate-induced currents in HEK293T cells either cotransfected with GluA1, GluA2, and stargazin (Fig. 6*A*) or cotransfected with GluA1 and stargazin (Fig. 6*B*). Not surprisingly, the currents were very small in the absence of stargazin, which is consistent with a previous report (16), although ABHD6 still significantly inhibited the peak amplitude and steady-state amplitude of ligand-induced currents (Fig. 6*C*). When stargazin alone was expressed in HEK293T cells, glutamate failed to elicit a detectable current, which is consistent with previous observations of HEK293T cells and *Xenopus* oocytes (7, 67, 68). ABHD6 transfection had no effects on membrane capacitance (control: 49 ± 3 pF; ABHD6: 48 ± 3 pF) or resistance (control: 785 ± 79 MΩ, n =172/18; ABHD6: 956 ± 72 MΩ, n =169/18), suggesting that these cells were normal. Thus, ABHD6 overexpression strongly inhibits AMPAR-mediated currents in HEK293T cells.

The observed reduction in AMPAR-mediated currents in the transfected HEK293T cells might have been because of the inhibition of surface-localized AMPA receptors, a decrease in the overall expression of GluAs, or an impairment in AMPAR trafficking to the surface. To distinguish between these possibilities, the total GluA1 levels were measured in HEK293T cells transfected with either GluA1 and stargazin alone or together with ABHD6. Quantitative immunoblotting revealed that ABHD6

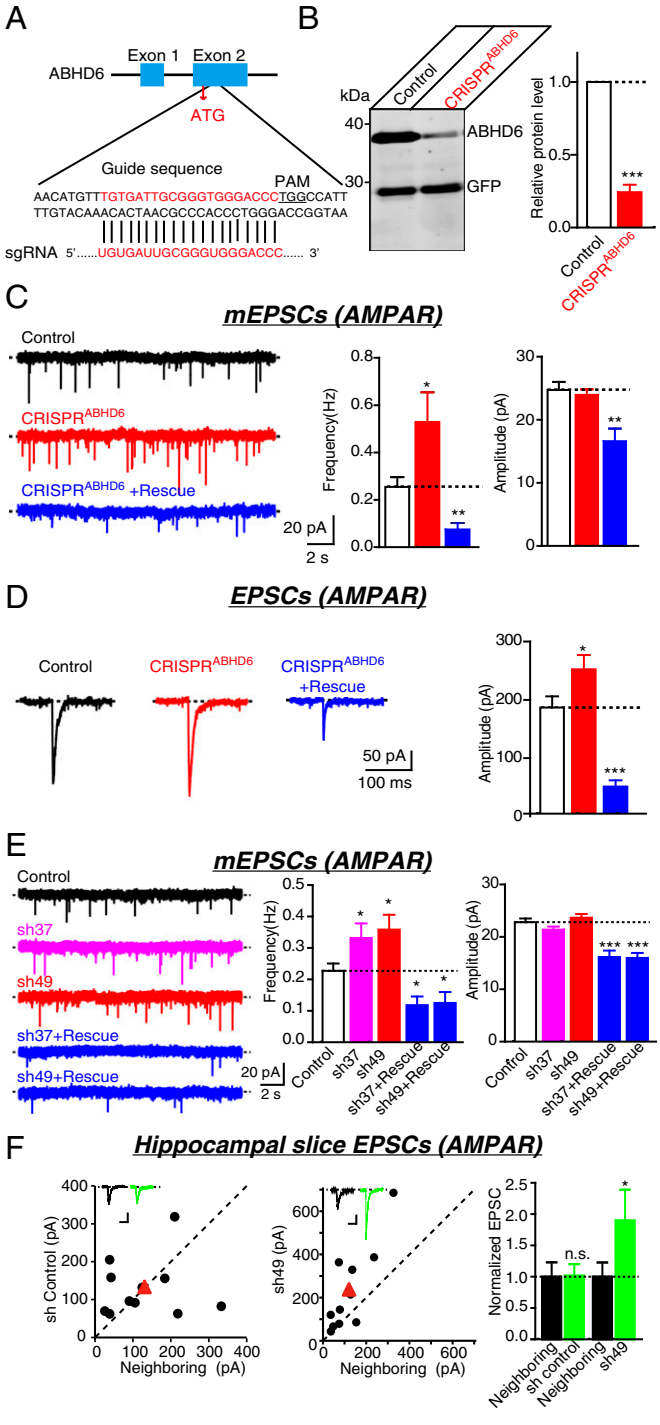

Fig. 5. Knockdown of ABHD6 by either CRISPR/Cas9 or shRNA increased AMPAR-mediated synaptic transmission. (*A*) Target sequence of CRISPR_ABHD6. (*B*) Representative immunoblot (*Left*) and quantitative graphs (*Right*) of proteins from HEK293T cells transfected with mouse ABHD6 together with either CRISPR_ABHD6 or control plasmids ($n = 4$; $^{***}P < 0.001$). (*C*) Representative traces (*Left*) and summary graphs of the frequencies (*Center*) and amplitudes (*Right*) of mEPSCs recorded from cultured hippocampal neurons transfected with either control plasmids, CRISPR_ABHD6, or CRISPR_ABHD6, together with rescue constructs in 1 μM TTX and 0.1 mM PTX (frequency: control: $n = 35/3$; CRISPR_ABHD6: $n = 34/3$, $^{*}P < 0.05$; CRISPR_ABHD6 + rescue: $n = 25/3$, $^{**}P < 0.01$; amplitude: control: $n = 32/3$; CRISPR_ABHD6: $n = 33/3$, $P > 0.05$; CRISPR_ABHD6 + rescue: $n = 8/3$, $^{**}P < 0.01$). (*D*) Representative traces (*Left*) and summary graphs of the amplitudes (*Right*) of action potential-evoked EPSCs recorded from cultured hippocampal neurons transfected with either control plasmids, CRISPR_ABHD6, or CRISPR_ABHD6, together with rescue constructs in 0.1 mM PTX (amplitude: control: $n = 48/5$; CRISPR_ABHD6: $n = 49/5$, $^{*}P < 0.05$; CRISPR_ABHD6 + rescue: $n = 27/5$, $^{***}P < 0.001$). (*E*) Representative traces (*Left*) and summary graphs of the frequencies (*Center*) and amplitudes (*Right*) of mEPSCs recorded from cultured hippocampal neurons transfected with control plasmids, sh37, sh49 alone or together with rescue constructs in 1 μM TTX and 0.1 mM PTX (frequency: control: $n = 107/12$; sh37: $n = 104/10$, $^{*}P < 0.05$; sh49: $n = 96/10$, $^{*}P < 0.05$; sh37+rescue: $n = 27/3$, $^{*}P < 0.05$; sh49+rescue: $n = 30/3$, $^{*}P < 0.05$; amplitude: control: $n = 101/12$; sh37: $n = 102/10$, $P > 0.05$; sh49: $n = 96/10$, $P > 0.05$; sh37+rescue: $n = 18/3$, $^{***}P < 0.001$; sh49+rescue: $n = 16/3$, $^{***}P < 0.001$). (*F*) The plots of the amplitude of AMPAR EPSCs of cells in acute hippocampal slices infected with AAVs expressing GFP (*Left*) or sh49 (*Center*) against the amplitudes of neighboring uninfected cells, and summary graphs of the normalized AMPAR EPSCs amplitude (*Right*). (*Inset*) Representative traces of synaptic responses during single AP stimulus (Scale bars in the *Left* and *Center* panels: 50 pA, 100 ms; control: $n = 11$, $P > 0.05$; sh49: $n = 11$; $^{*}P < 0.05$).

overexpression increased the total GluA1 protein level (Fig. S7). Quantitative immunostaining of GluA1 from permeabilized and nonpermeabilized transfected HEK293T cells revealed that the coexpression of ABHD6, GluA1, and stargazin reduced the surface expression of GluA1 compared with a control group (Fig. 6*D*). In addition, the total GluA1 immunostaining signal did not differ between the ABHD6 and control groups (Fig. 6*E*). This finding was consistent with the quantitative immunoblotting results, supporting the notion that ABHD6 inhibits AMPAR-mediated currents because of the selective reduction of surface-localized AMPARs.

The GluA1 C Terminus Mediated the Inhibitory Effect of ABHD6. To identify the essential region in the GluA1 for the inhibitory effect of ABHD6, we first investigated the subcellular localization of ABHD6. Two ABHD6 constructs were generated and tagged with an myc epitope on either the N terminus or the C terminus. Surface labeling of nonpermeabilized HEK293T cells revealed no surface expression of either the N-terminal or C-terminal tagged ABHD6 (Fig. 7 *A–D*), supporting the notion that ABHD6 is a membrane-bound cytoplasmic protein rather than a transmembrane protein (29). Therefore, the subcellular localization of ABHD6 implied that ABHD6 interacts with the C terminus of GluA1 because GluA1 itself is a transmembrane protein. To further test this hypothesis, we transfected HEK293T cells with plasmids expressing myc-tagged ABHD6 together with a full-length GluA1 or GluA1 deletion construct (Fig. 7*E*), and immunoprecipitated ABHD6 using anti-myc antibodies. We found that ABHD6 was specifically coimmunoprecipitated with GluA1 only when both ABHD6 and GluA1 were expressed. GluA1 C-terminal deletion ending with EFCYK-tag-stop (D15A1) (Fig. 7*E*) showed significantly less binding to ABHD6-myc (Fig. 7*F*). Quantitation of the bound proteins relative to the total input showed that D15A1 retained myc-ABHD6 with ~8 ± 6% of the efficiency of full-length GluA1, suggesting that ABHD6 binds to the GluA1 C terminus. Consequently, 15 GluA1 C-terminal deletion constructs were generated to more precisely identify the sequence required for this phenotype. A human influenza hemagglutinin (HA) tag was fused to the C termini of all of the constructs with a GQG spacer (Fig. 7*E*). When these constructs were cotransfected with stargazin into HEK293T cells, the AMPAR mutants D12A1, D13A1, D14A1, and D15A1 still exhibited robust glutamate-induced currents but were resistant to ABHD6 inhibition (Fig. 7*G*). Based on the results from deletion constructs, we further generated two mutation constructs [replacements of CLIPQ or GFCLIPQ sequence with AAAAA (M1A1) or AAAAAAA (M2A1), respectively] and examined whether ABHD6 still inhibited the ligand-gated currents in HEK293T cells expressing these mutation constructs. Our data showed that M1A1 and M2A1 significantly reduced the inhibitory effects of ABHD6 on the GluA1-mediated

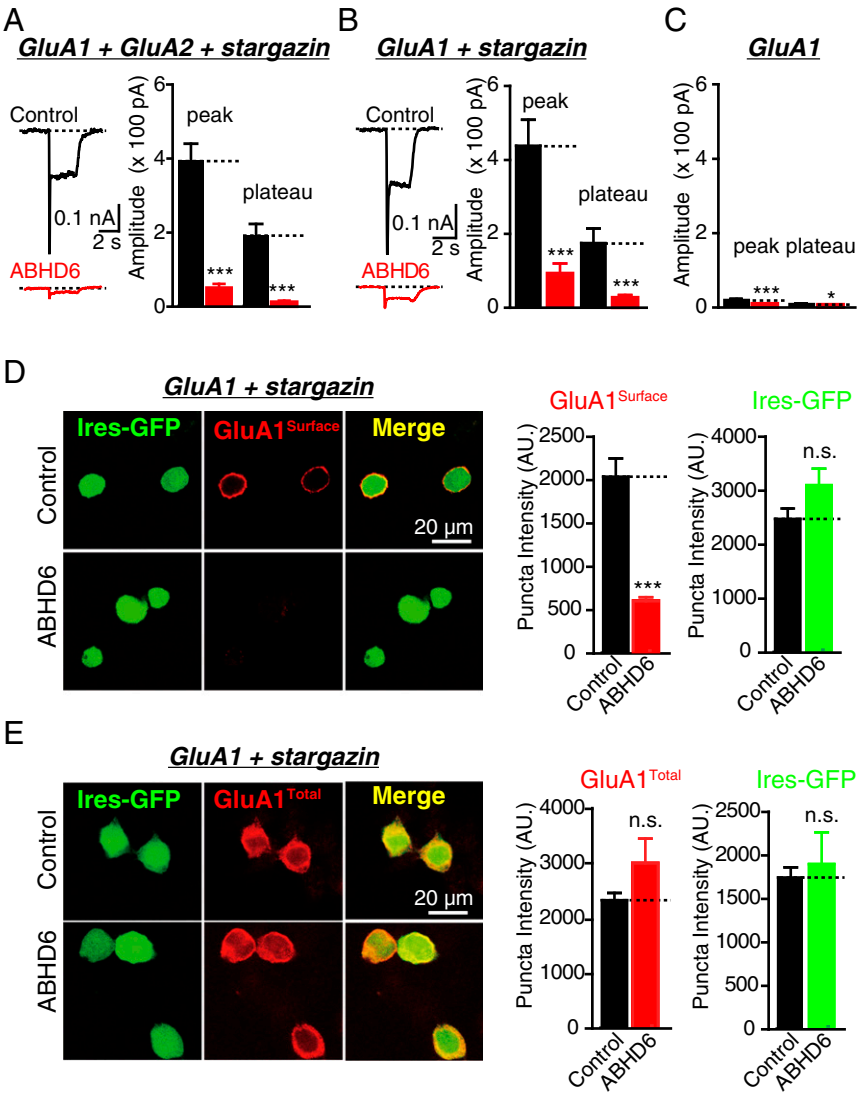

Fig. 6. Expression of ABHD6 reduced glutamate-induced currents and the surface expression of GluA1 in HEK293T cells. (*A*) Representative traces (*Left*) and peak amplitudes and plateaus (*Right*) of currents induced by the application of 10 mM GluK to HEK293T cells transfected with combinations of GluA1, GluA2, and stargazin (control: $n = 60/6$; ABHD6: $n = 60/6$; peak: $^{***}P < 0.001$; plateau: $^{***}P < 0.001$). (*B*) Representative traces (*Left*) and peak amplitudes and plateaus (*Right*) of currents induced by the application of 10 mM GluK to HEK293T cells transfected with combinations of GluA1 and stargazin (control: $n = 37/5$; ABHD6: $n = 34/5$; peak: $^{***}P < 0.001$; plateau: $^{***}P < 0.001$). (*C*) Representative traces (*Left*) and peak amplitudes and plateaus (*Right*) of currents induced by the application of 10 mM GluK to HEK293T cells transfected with GluA1 (control: $n = 20/3$; ABHD6: $n = 24/3$; peak: $^{***}P < 0.001$; plateau: $^{*}P < 0.05$). (*D*) Measurement of the surface expression of GluA1 in HEK293T cells expressing ABHD6 or a control plasmid together with GluA1 and stargazin. The transfected HEK293T cells were stained without permeabilization using an anti-GluA1 antibody. The panels show representative images (*Left*) and quantification of the puncta intensity (*Right*) (control: $n = 101/3$; ABHD6: $n = 100/3$; IRES-GFP: $P > 0.05$; $GluA1^{surface}$: $^{***}P < 0.001$). (*E*) Measurement of the total GluA1 in HEK293T cells expressing ABHD6 or a control plasmid together with GluA1 and stargazin. The transfected HEK293T cells were stained using an anti-GluA1 antibody. The panels show representative images (*Left*) and quantification of the puncta intensity (*Right*) (control: $n = 72/3$; ABHD6: $n = 72/3$; IRES-GFP: $P > 0.05$; $GluA1^{total}$: $P > 0.05$).

currents in the transfected HEK293T cells, and M2A1 showed a nearly complete "rescue" effect (Fig. 7*G*). Taking these data together, our results demonstrated that GFCLIPQ sequence in the GluA1 C terminus was required for the inhibitory effects of ABHD6 on AMPAR function in the transfected HEK293T cells.

The Inhibitory Effect of ABHD6 on AMPARs in Hippocampal Neurons and Transfected HEK293T Cells Was Independent of 2-AG Signaling. Because ABHD6 hydrolyzes 2-AG, ABHD6 may impair AMPAR-mediated currents through 2-AG signaling. To test this hypothesis, HEK293T cells were treated with 10 μM WWL70, a specific inhibitor of ABHD6 lipase activity (33, 69), and ligand-gated currents were measured in the presence of WWL70. In the presence of WWL70, ABHD6 overexpression suppressed glutamate-induced currents in HEK293T cells expressing GluA1, GluA2, and stargazin (19.17 ± 5.85%) (Fig. 8*A*), and in HEK293T cells expressing only GluA1 and stargazin (28.91 ± 7.56%). The level of suppression was similar to that observed in a dimethyl sulfoxide-treated control group (22.79 ± 6.99%). To confirm this observation, three previously characterized ABHD6 mutations that block the enzymatic activity of ABHD6 were generated, and the ability of these mutants to retain the inhibitory effects on glutamate-induced currents in the HEK293T overexpression system was tested. Based on a previous bioinformatics analysis of the ABHD gene family, the consensus active site motif for serine hydrolase is G-X-S-X-G in 12 of 15 ABHD genes, including ABHD6 (22). A biochemical study

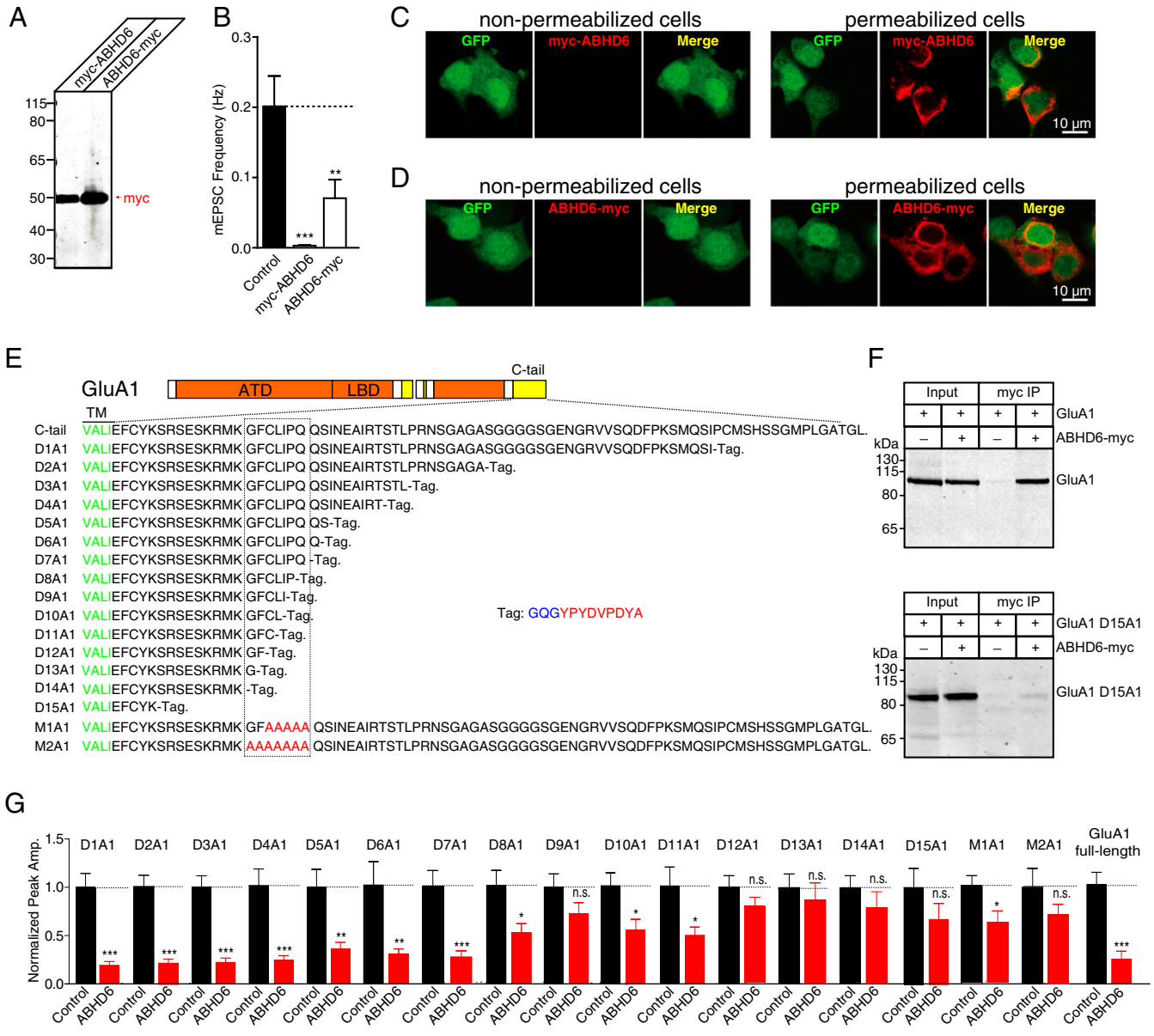

Fig. 7. A discrete cysteine-containing sequence in the GluA1 cytoplasmic region was required for the ABHD6-induced inhibition of AMPAR function. (*A*) Measurement of the expression of ABHD6 in HEK293T cells expressing the N-terminally or C-terminally myc-tagged ABHD6. (*B*) Summary graphs of the mean frequency of mEPSCs recorded from neurons transfected with a control vector and vectors encoding myc-ABHD6 (N-terminal myc-tag) or ABHD6-myc (C-terminal myc-tag) (control: 22/4; myc-ABHD6: 28/3, $^{**}P < 0.01$; ABHD6-myc: 29/3, $^{***}P < 0.001$). (*C* and *D*) Staining of ABHD6 in HEK293T cells expressing myc-ABHD6 (*C*) or ABHD6-myc (*D*) using an anti-myc tag antibody. (*E*) The amino acid sequences of different GluA1 deletion and mutation constructs. (*F*) Pull-down of HA-tagged GluA1 or D15-A1 expressed in transfected HEK293T cells coexpressing myc-tagged ABHD6 by an antibody against myc-tag. ABHD6 was immobilized by an anti-myc antibody immobilized onto protein G beads. Binding was visualized by immunoblotting for the HA-tag. (*G*) Summary graphs of the peak amplitudes of the currents induced by the application of 10 mM GluK to HEK293T cells transfected with different GluA1 deletions/mutations, stargazin, and a control vector or vectors encoding ABHD6 (D1A1, control: 24/3, ABHD6: 24/3, $^{***}P < 0.001$; D2A1, control: 24/3, ABHD6: 24/3, $^{***}P < 0.001$; D3A1, control: 23/3, ABHD6: 22/3, $^{***}P < 0.001$; D4A1, control: 24/3, ABHD6: 24/3, $^{***}P < 0.001$; D5A1, control: 28/3, ABHD6: 23/3, $^{**}P < 0.01$; D6A1, control: 27/3, ABHD6: 25/3, $^{**}P < 0.01$; D7A1, control: 27/3, ABHD6: 27/3, $^{***}P < 0.001$; D8A1, control: 44/5, ABHD6: 41/5, $^{*}P < 0.05$; D9A1, control: 32/4, ABHD6: 32/4, $P > 0.05$; D10A1, control: 24/3, ABHD6: 24/3, $^{*}P < 0.05$; D11A1, control: 24/3, ABHD6: 24/3, $^{*}P < 0.05$; D12A1, control: 36/4, ABHD6: 37/4, $P > 0.05$; D13A1, control: 27/3, ABHD6: 26/3, $P > 0.05$; D14A1, control: 27/3, ABHD6: 27/3, $P > 0.05$; D15A1, control: 28/3, ABHD6: 28/3, $P > 0.05$; M1A1, control: 45/5, ABHD6: 45/5, $^{*}P < 0.05$; M2A1, control: 28/3, ABHD6: 28/3, $P > 0.05$; GluA1 full-length, 61/8, ABHD6: 58/8, $^{***}P < 0.001$).

showed that S148 is essential for the enzymatic activity of ABHD6 (70). The same study also demonstrated that mutation of two other residues (D278 and H306) abolished the catalytic ability of ABHD6, although the introduction of these two mutations significantly decreased the expression of ABHD6 (70). Consistent with previous observations, the introduction of S148A into ABHD6 had no significant effect on ABHD6 protein expression levels in transfected HEK293T cells compared with wild-type ABHD6, whereas two other mutations (D278N and H306A) caused an ∼40% reduction in ABHD6 expression (Fig. S8). When the S148A and D278N mutants were coexpressed with GluA1 and stargazin in HEK293T cells, ligand-induced currents were still significantly reduced, reinforcing the notion

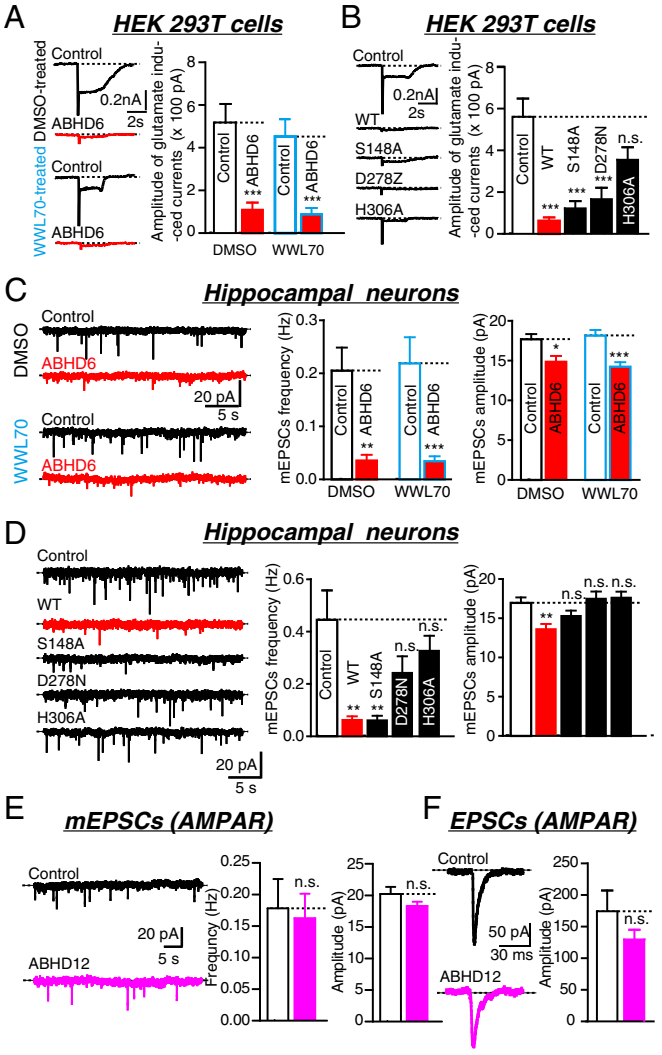

Fig. 8. Blocking the hydrolase activity of ABHD6 by mutagenesis or WWL70 treatment did not ablate the ABHD6-induced inhibition of AMPAR function in HEK293T cells and neurons. (*A*) Representative traces (*Left*) and summary graphs of the peak amplitudes (*Right*) of currents induced by the application of 10 mM GluK to HEK293T cells transfected with GluA1, GluA2, and stargazin, with either a control vector or a vector encoding ABHD6, with (WWL70, control: 24/3, ABHD6: 24/3; $***P < 0.001$) or without (DMSO, control: 24/3, ABHD6: 24/3; $***P < 0.001$) treatment with 10 μM WWL70. (*B*) Representative traces (*Left*) and summary graphs of the peak amplitudes (*Right*) of currents induced by the application of 10 mM GluK to HEK293T cells transfected with GluA1, GluA2, stargazin, and different mutations of ABHD6 (control: $n = 21/3$; wt: 21/3, $***P < 0.001$; S148A: 22/3, $***P < 0.001$; D278N: 22/3, $***P < 0.001$; H306A: 21/3, $P = 0.059$). (*C*) Representative traces (*Left*) and summary graphs of the mean frequencies (*Center*) and amplitudes (*Right*) of mEPSCs recorded from neurons transfected with a control vector or vectors encoding ABHD6 with (WWL70, frequency: control: 74/8, ABHD6: 73/8, $***P < 0.001$; amplitude: control: 71/8, 41/8, $***P < 0.001$) or without (DMSO, frequency: control: 45/5, ABHD6: 35/5, $**P < 0.01$; amplitude: control: 37/4, ABHD6: 19/4, $*P < 0.05$) treatment with WWL70 (10 μM). (*D*) Cultured hippocampal neurons transfected with either an empty vector (control) or a vector encoding ABHD6-2A-GFP (ABHD6), $ABHD6^{S148A}$-2A-GFP, $ABHD6^{D278N}$-2A-GFP, or $ABHD6^{H306A}$-2A-GFP. Representative traces (*Left*) and summary graphs of the mean frequencies (*Center*) and amplitudes (*Right*) of mEPSCs recorded in 1 μM TTX and 10 μM PTX (frequency: control: $n = 66/6$, wt: 44/6, $**P < 0.01$, S148A: 66/6, $***P < 0.001$, D278N: 50/6, $P > 0.05$, H306A: 55/6, $P > 0.05$; amplitude: control: 47/6, wt: 17/6, $**P < 0.01$, S148A: 16/6, $P > 0.05$, D278N: 32/6, $P > 0.05$, H306A: 39/6, $P > 0.05$). (*E*) Representative traces (*Left*) and summary graphs of the frequencies (*Center*) and amplitudes (*Right*) of mEPSCs recorded in 1 μM tetrodotoxin (TTX) and 0.1 mM PTX (frequency: control: $n = 37$ cells/4 cultures; ABHD6: $n = 33/4$, $P > 0.05$, amplitude: $n = 32$ cells/4 cultures; ABHD6: $n = 26/4$, $P > 0.05$). (*F*) Representative traces (*Left*) and summary graphs of the amplitude (*Center*) of action potential-evoked EPSCs recorded in 0.1 mM PTX (control: $n = 28/3$; ABHD6: $n = 25/3$; $P > 0.05$).

that 2-AG signaling was dispensable in the inhibitory effects of ABHD6 on AMPARs (Fig. 8*B*).

To examine whether ABHD6 affected AMPARs in neurons by altering endocannabinoid signaling via its enzymatic activity (breaking down 2-AG), the same three sets of experiments as we performed in HEK293T cells were performed. First, neurons were incubated with WWL70 after 10 DIV to block the lipase activity of ABHD6. mEPSCs were recorded after 14 DIV. The results showed that the WWL70 treatment did not affect the mEPSC phenotype caused by ABHD6 overexpression (Fig. 8*C*). Second, lipase-deficient mutants were transfected into hippocampal neurons. Again, the S148A mutant significantly reduced the frequency of mEPSCs, similar to the effect observed in wild-type ABHD6 (Fig. 8*D*). The D278N and H306A mutants showed a trend toward a reduction in mEPSC frequency, although this was not significant, likely because of the reduction in ABHD6 protein levels, as demonstrated in Fig. S8. Finally, ABHD12, another lipase that hydrolyzes 2-AG in the brain, was overexpressed in hippocampal neurons, and the mEPSCs and EPSCs mediated by AMPARs were monitored. In contrast to the effect of ABHD6 overexpression, ABHD12 overexpression did not affect mEPSCs or AP-evoked EPSCs (Fig. 8 *E* and *F*). Thus, consistent with the observations in HEK293T cells, ABHD6 affects synaptic AMPARs in neurons in a 2-AG–independent and highly specific manner.

Discussion

AMPARs are the major postsynaptic receptors that mediate excitatory synaptic transmission. Although researchers have discovered many auxiliary proteins in the past decade, the specific roles of these putative interacting proteins in regulating the function of AMPARs remain to be elucidated. ABHD6 has been found in AMPAR macromolecular complexes (21). As demonstrated in the present study, ABHD6 specifically decreased the surface expression of postsynaptic AMPARs via a hydrolase-independent mechanism. The three principal observations of this study are as follows.

First, ABHD6 was physiologically and functionally involved in the function of the AMPARs at synapses, as supported by: (*i*) the loss of ABHD6 in cultured neurons or in brain slices increased AMPAR-mediated synaptic transmission (Fig. 5); (*ii*) overexpression of ABHD6 in dissociated hippocampal neurons or in brain slices decreased AMPAR-mediated synaptic transmission (Fig. 1) and postsynaptic surface AMPARs (Fig. 3); and (*iii*) overexpression of ABHD6 in transfected HEK293T cells decreased AMPAR-mediated ligand-gated currents and the surface expression of AMPARs (Fig. 6). The effect of ABHD6 was dramatic in all three systems and was consistent across different experiments, as indicated by the 75–95% reduction in mEPSC frequency caused by ABHD6 overexpression (Fig. S9). ABHD6 expression almost abolished ligand-gated AMPAR-mediated currents in the HEK293T cells and neurons. Furthermore, both the peak and plateau amplitudes of glutamate-induced currents were affected in the HEK293T and neuronal cells. The effect was specific at AMPAR-containing synapses; there were no changes in GABAR- or NMDAR-mediated synaptic transmission (Fig. 2). The loss-of-function analysis showed that inactivation of ABHD6 expression in cultured hippocampal neurons or in brain slices increased AMPAR-mediated excitatory neurotransmission (Fig. 5), further supporting the notion that ABHD6

is physiologically and functionally involved in the function of AMPARs at synapses.

Second, ABHD6 inhibited the function of AMPARs by decreasing the surface expression of the receptors. The surface-labeling experiments showed that overexpression of ABHD6 selectively inhibited the surface delivery of AMPARs. However, ABHD6 overexpression had no effect on the total expression levels of GluA in transfected HEK293T cells (Fig. 6) or on the total postsynaptic GluA1 levels, as revealed by immunostaining of transfected neurons (Fig. 3). Furthermore, overexpression ABHD6 in hippocampal CA1 neurons reduced the pairing LTP (Fig. 4), suggesting that ABHD6 is involved in both constitutive and activity-dependent receptor trafficking. These observations suggest that ABHD6 functions during receptor trafficking.

Third, ABHD6-induced inhibition of the function of AMPARs was independent of 2-AG signaling. This conclusion was supported by the observations that WWL70 treatment and hydrolase-deficient mutants did not rescue the ABHD6-induced suppression of AMPAR-mediated mEPSCs. The finding that neither WWL70 treatment nor the transfection of various ABHD6 hydrolase-deficient mutants into HEK293T cells expressing GluA with stargazin affected the phenotype of ABHD6 (Fig. 8) further strengthened this conclusion.

Physiological Significance. The data clearly showed that ABHD6 functionally interacted with AMPARs and selectively decreased the surface expression—but not the overall expression levels—of AMPARs. Thus, the striking effects observed in these experiments perhaps reflect a direct functional interaction between ABHD6 and AMPARs in addition to the previously reported physical association (21). In contrast to stargazin (γ-2), which promotes AMPAR trafficking to the plasma membrane (15, 16, 71), ABHD6 serves as a negative regulator in this process. A key observation in the present study was that the expression of ABHD6 in hippocampal neurons or in brain slices suppressed synaptic AMPARs in a cell-autonomous manner, corroborating the role of ABHD6 as a key negative regulator of synaptic AMPARs. This potential role of ABHD6 was further strengthened by the finding that deletion of ABHD6 in cultured hippocampal neurons or in brain slices increased AMPAR-mediated neurotransmission (Fig. 5).

This inhibitory effect is mostly a postsynaptic phenomenon. This occurred for the following three reasons: (*i*) The number of excitatory synapses, measured as the number of PSD-95$^+$, vGlut1$^+$, or GluA1$^+$ puncta, was not reduced in neurons overexpressing ABHD6 (Fig. 3); (*ii*) the NMDAR-mediated synaptic response was not affected by ABHD6 overexpression (Fig. 2), suggesting that the excitatory synapses had normal presynaptic transmitter release; and (*iii*) the paired-pulse ratio was normal in AMPAR-mediated (Fig. S10) or NMDAR-mediated (Fig. 2*E*) synaptic transmission in ABHD6-overexpressing neurons, excluding the possibility of ABHD6 involvement in the release probability. Thus, ABHD6 specifically affects postsynaptic AMPAR to mediate its inhibitory effect on glutamatergic synaptic transmission.

We propose that the effect of ABHD6 on postsynaptic AMPARs is independent of its hydrolase activity on 2-AG. This theory appears to contradict the well-known lipase function of ABHD6. However, the lipase function of ABHD6 may be more apparent than real. 2-AG is produced and released from postsynaptic neurons and subsequently binds to presynaptic endocannabinoid receptors to inhibit vesicle fusion. Thus, the activation of 2-AG–endocannabinoid pathways mainly serves to prevent strong stimulation by decreasing presynaptic transmitter release to maintain synaptic homeostasis (39, 72–77). MAGL, ABHD6, and ABHD12 hydrolyze almost 99% of the 2-AG in the brain, with ABHD6 accounting for less than 5% of the hydrolase activity (mainly in neurons) (33, 78). Pharmacological blockade of ABHD6 in cortical slices had a small but significant effect on cannabinoid receptor type 1-dependent long-term depression. In the present study, the postsynaptic expression of ABHD6 or ABHD6 hydrolase-deficient mutations significantly reduced the surface expression of AMPARs and inhibited AMPAR-mediated synaptic transmission. These effects were independent of the hydrolase activity of ABHD6. These findings reveal a previously unknown function of ABHD6: it acts on postsynaptic AMPARs. This role complements the hydrolase activity of ABHD6, which is thought to target presynaptic transmitter release.

Furthermore, a number of unanswered questions remain for future investigations. We found that ABHD6 binds to the C terminus of GluA1, and a GFCLIPQ sequence in the C terminus of GluA1 was required for the inhibitory effect of ABHD6 (Fig. 7); this finding may represent a starting point for further investigations on the underlying mechanisms. Although constitutive and activity-dependent AMPAR trafficking is controlled by different mechanisms (79–81), overexpression of ABHD6 decreases the amplitude of evoked EPSCs and LTP. Thus, resolving the mechanism underlying the inhibitory effects of ABHD6 will help elucidate the functional importance of the ABHD6–AMPAR interaction within the framework of the mechanisms currently known to regulate the functions of AMPARs at synapses.

Materials and Methods

Vector construction, cell culture, transfection, electrophysiology, protein purification, Western blotting, and immunostaining experiments are described in detail in *SI Materials and Methods*.

All animal experiments were performed in accordance with the *Guide for the Care and Use of Laboratory Animals* (Eighth edition) (82). All experimental protocols were approved by the Institutional Animal Care and Use Committee of Peking University.

For all representative data, scale bars apply to all panels in a set. All summary graphs show the means ± SEMs; statistical comparisons via Student's *t* test yielded $*P < 0.05$, $**P < 0.01$, and $***P < 0.001$.

ACKNOWLEDGMENTS. We thank Dr. Thomas C. Südof for beneficial discussions and critical comments on the manuscript, and S. Y. Liu for technical support. This work was supported by grants from the National Basic Research Program of China (Grants 2014CB942804, 2012YQ0302604 and 2014BAI03B01), the National Science Foundation of China (Grants 31222025 and 31171025), Beijing Institute of Collaborative Innovation (Grant 15I-15-BJ), and the Seeding Grant for Medicine and Life Sciences of Peking University (Grant 2014-MB-11).

1. Borges K, Dingledine R (1998) AMPA receptors: Molecular and functional diversity. *Prog Brain Res* 116:153–170.
2. Bettler B, Mulle C (1995) Review: Neurotransmitter receptors. II. AMPA and kainate receptors. *Neuropharmacology* 34(2):123–139.
3. Hollmann M, Heinemann S (1994) Cloned glutamate receptors. *Annu Rev Neurosci* 17: 31–108.
4. Mayer ML (2006) Glutamate receptors at atomic resolution. *Nature* 440(7083): 456–462.
5. Wu TY, Liu CI, Chang YC (1996) A study of the oligomeric state of the alpha-amino-3-hydroxy-5-methyl-4-isoxazolepropionic acid-preferring glutamate receptors in the synaptic junctions of porcine brain. *Biochem J* 319(Pt 3):731–739.
6. Rosenmund C, Stern-Bach Y, Stevens CF (1998) The tetrameric structure of a glutamate receptor channel. *Science* 280(5369):1596–1599.
7. Shi Y, et al. (2010) Functional comparison of the effects of TARPs and cornichons on AMPA receptor trafficking and gating. *Proc Natl Acad Sci USA* 107(37):16315–16319.
8. Shi Y, Lu W, Milstein AD, Nicoll RA (2009) The stoichiometry of AMPA receptors and TARPs varies by neuronal cell type. *Neuron* 62(5):633–640.
9. Kato AS, Siuda ER, Nisenbaum ES, Bredt DS (2008) AMPA receptor subunit-specific regulation by a distinct family of type II TARPs. *Neuron* 59(6):986–996.
10. Tomita S, Fukata M, Nicoll RA, Bredt DS (2004) Dynamic interaction of stargazin-like TARPs with cycling AMPA receptors at synapses. *Science* 303(5663):1508–1511.
11. Opazo P, et al. (2010) CaMKII triggers the diffusional trapping of surface AMPARs through phosphorylation of stargazin. *Neuron* 67(2):239–252.
12. Tomita S, Sekiguchi M, Wada K, Nicoll RA, Bredt DS (2006) Stargazin controls the pharmacology of AMPA receptor potentiators. *Proc Natl Acad Sci USA* 103(26): 10064–10067.
13. Tomita S, et al. (2005) Stargazin modulates AMPA receptor gating and trafficking by distinct domains. *Nature* 435(7045):1052–1058.
14. Vandenberghe W, Nicoll RA, Bredt DS (2005) Stargazin is an AMPA receptor auxiliary subunit. *Proc Natl Acad Sci USA* 102(2):485–490.

15. Chen L, El-Husseini A, Tomita S, Bredt DS, Nicoll RA (2003) Stargazin differentially controls the trafficking of alpha-amino-3-hydroxyl-5-methyl-4-isoxazolepropionate and kainate receptors. *Mol Pharmacol* 64(3):703–706.
16. Chen L, et al. (2000) Stargazin regulates synaptic targeting of AMPA receptors by two distinct mechanisms. *Nature* 408(6815):936–943.
17. Brockie PJ, et al. (2013) Cornichons control ER export of AMPA receptors to regulate synaptic excitability. *Neuron* 80(1):129–142.
18. Coombs ID, et al. (2012) Cornichons modify channel properties of recombinant and glial AMPA receptors. *J Neurosci* 32(29):9796–9804.
19. Shanks NF, et al. (2012) Differences in AMPA and kainate receptor interactomes facilitate identification of AMPA receptor auxiliary subunit GSG1L. *Cell Reports* 1(6): 590–598.
20. von Engelhardt J, et al. (2010) CKAMP44: A brain-specific protein attenuating short-term synaptic plasticity in the dentate gyrus. *Science* 327(5972):1518–1522.
21. Schwenk J, et al. (2012) High-resolution proteomics unravel architecture and molecular diversity of native AMPA receptor complexes. *Neuron* 74(4):621–633.
22. Lefèvre C, et al. (2001) Mutations in CGI-58, the gene encoding a new protein of the esterase/lipase/thioesterase subfamily, in Chanarin-Dorfman syndrome. *Am J Hum Genet* 69(5):1002–1012.
23. Edgar AJ, Polak JM (2002) Cloning and tissue distribution of three murine alpha/beta hydrolase fold protein cDNAs. *Biochem Biophys Res Commun* 292(3):617–625.
24. Zhao S, et al. (2014) α/β-Hydrolase domain-6-accessible monoacylglycerol controls glucose-stimulated insulin secretion. *Cell Metab* 19(6):993–1007.
25. Li F, Fei X, Xu J, Ji C (2009) An unannotated alpha/beta hydrolase superfamily member, ABHD6 differentially expressed among cancer cell lines. *Mol Biol Rep* 36(4): 691–696.
26. Dinh TP, et al. (2002) Brain monoglyceride lipase participating in endocannabinoid inactivation. *Proc Natl Acad Sci USA* 99(16):10819–10824.
27. Gulyas AI, et al. (2004) Segregation of two endocannabinoid-hydrolyzing enzymes into pre- and postsynaptic compartments in the rat hippocampus, cerebellum and amygdala. *Eur J Neurosci* 20(2):441–458.
28. Straiker A, et al. (2009) Monoacylglycerol lipase limits the duration of endocannabinoid-mediated depolarization-induced suppression of excitation in autaptic hippocampal neurons. *Mol Pharmacol* 76(6):1220–1227.
29. Marrs WR, et al. (2010) The serine hydrolase ABHD6 controls the accumulation and efficacy of 2-AG at cannabinoid receptors. *Nat Neurosci* 13(8):951–957.
30. Long LE, Lind J, Webster M, Weickert CS (2012) Developmental trajectory of the endocannabinoid system in human dorsolateral prefrontal cortex. *BMC Neurosci* 13:87.
31. Max D, Hesse M, Volkmer I, Staege MS (2009) High expression of the evolutionarily conserved alpha/beta hydrolase domain containing 6 (ABHD6) in Ewing tumors. *Cancer Sci* 100(12):2383–2389.
32. Savinainen JR, et al. (2014) Robust hydrolysis of prostaglandin glycerol esters by human monoacylglycerol lipase (MAGL). *Mol Pharmacol* 86(5):522–535.
33. Blankman JL, Simon GM, Cravatt BF (2007) A comprehensive profile of brain enzymes that hydrolyze the endocannabinoid 2-arachidonoylglycerol. *Chem Biol* 14(12): 1347–1356.
34. Thomas G, et al. (2013) The serine hydrolase ABHD6 Is a critical regulator of the metabolic syndrome. *Cell Reports* 5(2):508–520.
35. Kreitzer AC, Regehr WG (2001) Retrograde inhibition of presynaptic calcium influx by endogenous cannabinoids at excitatory synapses onto Purkinje cells. *Neuron* 29(3): 717–727.
36. Wilson RI, Nicoll RA (2001) Endogenous cannabinoids mediate retrograde signalling at hippocampal synapses. *Nature* 410(6828):588–592.
37. Trettel J, Levine ES (2003) Endocannabinoids mediate rapid retrograde signaling at interneuron right-arrow pyramidal neuron synapses of the neocortex. *J Neurophysiol* 89(4):2334–2338.
38. Yanovsky Y, Mades S, Misgeld U (2003) Retrograde signaling changes the venue of postsynaptic inhibition in rat substantia nigra. *Neuroscience* 122(2):317–328.
39. Melis M, et al. (2004) Endocannabinoids mediate presynaptic inhibition of glutamatergic transmission in rat ventral tegmental area dopamine neurons through activation of CB1 receptors. *J Neurosci* 24(1):53–62.
40. Di S, et al. (2005) Activity-dependent release and actions of endocannabinoids in the rat hypothalamic supraoptic nucleus. *J Physiol* 569(Pt 3):751–760.
41. Zhong P, et al. (2011) Genetic deletion of monoacylglycerol lipase alters endocannabinoid-mediated retrograde synaptic depression in the cerebellum. *J Physiol* 589(Pt 20):4847–4855.
42. Straiker A, Mackie K (2009) Cannabinoid signaling in inhibitory autaptic hippocampal neurons. *Neuroscience* 163(1):190–201.
43. Straiker A, et al. (2011) COX-2 and fatty acid amide hydrolase can regulate the time course of depolarization-induced suppression of excitation. *Br J Pharmacol* 164(6): 1672–1683.
44. Bowman AL, Makriyannis A (2013) Highly predictive ligand-based pharmacophore and homology models of ABHD6. *Chem Biol Drug Des* 81(3):382–388.
45. Alhouayek M, Masquelier J, Cani PD, Lambert DM, Muccioli GG (2013) Implication of the anti-inflammatory bioactive lipid prostaglandin D2-glycerol ester in the control of macrophage activation and inflammation by ABHD6. *Proc Natl Acad Sci USA* 110(43): 17558–17563.
46. Feledziak M, Lambert DM, Marchand-Brynaert J, Muccioli GG (2012) Inhibitors of the endocannabinoid-degrading enzymes, or how to increase endocannabinoid's activity by preventing their hydrolysis. *Recent Patents CNS Drug Discov* 7(1):49–70.
47. Tchantchou F, Zhang Y (2013) Selective inhibition of alpha/beta-hydrolase domain 6 attenuates neurodegeneration, alleviates blood brain barrier breakdown, and improves functional recovery in a mouse model of traumatic brain injury. *J Neurotrauma* 30(7):565–579.
48. Naydenov AV, et al. (2014) ABHD6 blockade exerts antiepileptic activity in PTZ-induced seizures and in spontaneous seizures in R6/2 mice. *Neuron* 83(2):361–371.
49. Zhang C, et al. (2010) Neurexins physically and functionally interact with GABA(A) receptors. *Neuron* 66(3):403–416.
50. Incontro S, Asensio CS, Edwards RH, Nicoll RA (2014) Efficient, complete deletion of synaptic proteins using CRISPR. *Neuron* 83(5):1051–1057.
51. Laube B, Hirai H, Sturgess M, Betz H, Kuhse J (1997) Molecular determinants of agonist discrimination by NMDA receptor subunits: Analysis of the glutamate binding site on the NR2B subunit. *Neuron* 18(3):493–503.
52. Moriyoshi K, et al. (1991) Molecular cloning and characterization of the rat NMDA receptor. *Nature* 354(6348):31–37.
53. Vargas-Caballero M, Robinson HP (2004) Fast and slow voltage-dependent dynamics of magnesium block in the NMDA receptor: The asymmetric trapping block model. *J Neurosci* 24(27):6171–6180.
54. Granger AJ, Shi Y, Lu W, Cerpas M, Nicoll RA (2013) LTP requires a reserve pool of glutamate receptors independent of subunit type. *Nature* 493(7433):495–500.
55. Pennisi E (2013) The CRISPR craze. *Science* 341(6148):833–836.
56. Barrangou R, et al. (2007) CRISPR provides acquired resistance against viruses in prokaryotes. *Science* 315(5819):1709–1712.
57. Friedland AE, et al. (2013) Heritable genome editing in *C. elegans* via a CRISPR-Cas9 system. *Nat Methods* 10(8):741–743.
58. Cong L, et al. (2013) Multiplex genome engineering using CRISPR/Cas systems. *Science* 339(6121):819–823.
59. Mali P, et al. (2013) RNA-guided human genome engineering via Cas9. *Science* 339(6121):823–826.
60. Hwang WY, et al. (2013) Efficient genome editing in zebrafish using a CRISPR-Cas system. *Nat Biotechnol* 31(3):227–229.
61. Jiang W, Bikard D, Cox D, Zhang F, Marraffini LA (2013) RNA-guided editing of bacterial genomes using CRISPR-Cas systems. *Nat Biotechnol* 31(3):233–239.
62. Cho SW, Kim S, Kim JM, Kim JS (2013) Targeted genome engineering in human cells with the Cas9 RNA-guided endonuclease. *Nat Biotechnol* 31(3):230–232.
63. Jinek M, et al. (2013) RNA-programmed genome editing in human cells. *eLife* 2:e00471.
64. DiCarlo JE, et al. (2013) Genome engineering in *Saccharomyces cerevisiae* using CRISPR-Cas systems. *Nucleic Acids Res* 41(7):4336–4343.
65. Chang N, et al. (2013) Genome editing with RNA-guided Cas9 nuclease in zebrafish embryos. *Cell Res* 23(4):465–472.
66. Vandenberghe W, Nicoll RA, Bredt DS (2005) Interaction with the unfolded protein response reveals a role for stargazin in biosynthetic AMPA receptor transport. *J Neurosci* 25(5):1095–1102.
67. Yamazaki M, et al. (2004) A novel action of stargazin as an enhancer of AMPA receptor activity. *Neurosci Res* 50(4):369–374.
68. Strutz-Seebohm N, et al. (2006) Additive regulation of GluR1 by stargazin and serum- and glucocorticoid-inducible kinase isoform SGK3. *Pflugers Arch* 452(3):276–282.
69. Li W, Blankman JL, Cravatt BF (2007) A functional proteomic strategy to discover inhibitors for uncharacterized hydrolases. *J Am Chem Soc* 129(31):9594–9595.
70. Navia-Paldanius D, Savinainen JR, Laitinen JT (2012) Biochemical and pharmacological characterization of human α/β-hydrolase domain containing 6 (ABHD6) and 12 (ABHD12). *J Lipid Res* 53(11):2413–2424.
71. Tomita S, et al. (2003) Functional studies and distribution define a family of transmembrane AMPA receptor regulatory proteins. *J Cell Biol* 161(4):805–816.
72. Li Q, Yan H, Wilson WA, Swartzwelder HS (2010) Modulation of NMDA and AMPA-mediated synaptic transmission by CB1 receptors in frontal cortical pyramidal cells. *Brain Res* 1342:127–137.
73. Wang XH, et al. (2016) Cannabinoid CB1 receptor signaling dichotomously modulates inhibitory and excitatory synaptic transmission in rat inner retina. *Brain Struct Funct* 221(1):301–316.
74. Kushmerick C, et al. (2004) Retroinhibition of presynaptic Ca2+ currents by endocannabinoids released via postsynaptic mGluR activation at a calyx synapse. *J Neurosci* 24(26):5955–5965.
75. Brown SP, Brenowitz SD, Regehr WG (2003) Brief presynaptic bursts evoke synapse-specific retrograde inhibition mediated by endogenous cannabinoids. *Nat Neurosci* 6(10):1048–1057.
76. Morisset V, Urban L (2001) Cannabinoid-induced presynaptic inhibition of glutamatergic EPSCs in substantia gelatinosa neurons of the rat spinal cord. *J Neurophysiol* 86(1):40–48.
77. Kano M, Ohno-Shosaku T, Hashimotodani Y, Uchigashima M, Watanabe M (2009) Endocannabinoid-mediated control of synaptic transmission. *Physiol Rev* 89(1): 309–380.
78. Savinainen JR, Saario SM, Laitinen JT (2012) The serine hydrolases MAGL, ABHD6 and ABHD12 as guardians of 2-arachidonoylglycerol signalling through cannabinoid receptors. *Acta Physiol (Oxf)* 204(2):267–276.
79. Derkach VA, Oh MC, Guire ES, Soderling TR (2007) Regulatory mechanisms of AMPA receptors in synaptic plasticity. *Nat Rev Neurosci* 8(2):101–113.
80. Malinow R, Malenka RC (2002) AMPA receptor trafficking and synaptic plasticity. *Annu Rev Neurosci* 25:103–126.
81. Malenka RC (2003) Synaptic plasticity and AMPA receptor trafficking. *Ann N Y Acad Sci* 1003:1–11.
82. National Research Council of the National Academies (2011) *Guide for the Care and Use of Laboratory Animals,* Eighth ed. (National Academies Press, Washington, DC).
83. Maximov A, Pang ZP, Tervo DG, Südhof TC (2007) Monitoring synaptic transmission in primary neuronal cultures using local extracellular stimulation. *J Neurosci Methods* 161(1):75–87.